

# Physics of a two-temperature thermonuclear burning wave in an inertially confined plasma

S. Yu. Gus'kov, D. V. Il'in, A. A. Levkovskii, and V. E. Sherman

*Leningrad Machine-Building Institute, 195108 St. Petersburg, Russia*

N. V. Zmitrenko

*Institute of Mathematical Modeling, RAS, 125047 Moscow, Russia*

V. B. Rozanov

*P. N. Lebedev Physics Institute, 117924 Moscow, Russia*

(Submitted 19 May 1994)

Zh. Eksp. Teor. Fiz. **106**, 1069–1088 (October 1994)

Results are presented from numerical and analytical simulation of the propagation of a spherical thermonuclear burning wave in a plasma target used in laser thermonuclear fusion. The numerical simulation of the fast-particle kinetics was done using the Monte Carlo method. Estimates are found for the relative contributions of the different energy transport mechanisms for various plasma parameters. In the stage of a fully-developed burning wave, when numerical calculations reveal that ion-electron exchange is small, self-similar solutions are found for the thermonuclear burning wave in a dense spherical two-temperature plasma. The different self-similar burning regimes are classified and conditions are found for them to occur as a function of the plasma parameters behind the wave front. © 1994 American Institute of Physics.

## 1. INTRODUCTION

The efficiency of an inertially confined fusion (ICF) target is characterized by the gain coefficient  $K = E_f/E_d$ , where  $E_f$  is the energy produced in the target as a result of thermonuclear reactions and  $E_d$  is the energy of the external source (driver) acting on the target. A high value of  $K$  can be achieved by initiating a self-sustaining thermonuclear burning wave propagating from the hot central region of the plasma through the surrounding cold fuel. In fact, in spatially uniform burning of a DT plasma the gain coefficient does not exceed  $\sim 20$ – $50$ . But if a burning wave develops in a non-uniform plasma this can enhance  $K$  by a factor equal to the ratio of the mass of the cold fuel to that of the hot region in which the burn originally occurs. Such nonuniform burning regimes have been found repeatedly in numerical simulation of laser targets.<sup>1–3</sup> In these calculations values  $K \geq 100$  were achieved with laser radiation of wavelength  $\lambda \leq 1 \mu\text{m}$  for energies exceeding a few megajoules ( $2$ – $7 \text{ MJ}$ , depending on  $\lambda$ ).

Thus, the development of a thermonuclear burning wave is one of the most important and interesting problems in the physics of ICF targets. To study this problem requires a self-consistent solution of the system of equations for the plasma hydrodynamics and the kinetic equations for the thermonuclear particles. The mathematical complexity of the problem, on the one hand, and the need to determine the functional dependence of the thermonuclear burning process on the target parameters on the other make it useful to employ a combined numerical-analytical approach. The numerical calculations of the thermonuclear burning wave in the present wave were performed using the TERA code,<sup>4–6</sup> designed for the simultaneous solution of the equations of two-

temperature plasma hydrodynamics with electron thermal conductivity and the kinetic equations for neutral and charged thermonuclear particles. The numerical solution of the kinetic equations for the thermonuclear particles in the TERA code is based on the use of a Monte Carlo technique.

Our numerical calculations reveal that two characteristic stages can be distinguished in the development of a thermonuclear burning wave. The first stage is that in which the wave forms; it is characterized by a low propagation speed and a temperature which falls off or grows slowly behind the front. The second stage is that in which the wave is fully developed; it is characterized by a rapid rise in temperature and a fast rate of propagation, greater than the speed at which the target expands and the speed of sound behind the front. In this stage the intensity of ion-electron energy exchange is reduced, and a two-temperature plasma develops.

The analytical solutions of the problem found in the literature for a thermonuclear burning wave in a bounded plasma apply to the description of the initial one-temperature stage of the process. In Refs. 7–14 approximate solutions for different energy transport mechanisms, such as electron thermal conduction,<sup>7–9</sup> conduction by  $\alpha$  particles,<sup>8–11</sup> and detonation<sup>12</sup> were constructed in the case of a partially non-uniform plasma (one in which the temperature varied spatially). In Refs. 8 and 9 self-similar solutions of the problem were derived for the general case of a nonuniform plasma (variable temperature and density). Some self-similar solutions for two regimes in which thermonuclear burning waves propagate (sub- and supersonic) were treated in Refs. 13 and 14. We note also the treatment in Ref. 15, in which the self-similar solutions of the quasilinear thermal conduction equation were classified.

The present work is devoted to the analytical investiga-

tion of the processes by which thermonuclear burning waves propagate in a dense spherical two-temperature plasma in the stage in which intense energy production occurs, using self-similar solutions. The problem was formulated and the approximate mathematical physics of the thermonuclear burning wave was chosen on the basis of a set of numerical calculations of the ICF target burning dynamics carried out using the TERA code.

## 2. NUMERICAL CALCULATIONS OF THE BURNING WAVE IN A LASER THERMONUCLEAR TARGET

### 2.1. Choosing the approximate model

The mathematical model of the thermonuclear burning problem in a spherical target employed in the TERA code is described by the equations of energy balance and motion, together with the equations of state, continuity, and the quasisteady kinetic equations for fast thermonuclear particles.<sup>5,6</sup> In the Lagrangian coordinate system  $dm = \rho(r)r^2 dr$  [here  $\rho(r)$  is the plasma density] the Euler equation for two-temperature one-fluid hydrodynamics can be written in the form

$$\frac{1}{r^2} \frac{\partial u}{\partial t} = -\frac{\partial P}{\partial m} + \frac{VF}{r^2}. \quad (1)$$

Here  $u(r,t)$  is the local material velocity,  $V(r,t) = 1/\rho(r,t)$  is the plasma specific volume,  $P(r,t) = P_i + P_e$  is the total of the ion and electron pressures, and  $F(r,t)$  is the pressure force due to fast thermonuclear particles.

We describe mass transport by means of the continuity equation, taking into account burnup, losses, and thermalization of the reaction products:<sup>5</sup>

$$\frac{\partial V}{\partial t} = \frac{\partial}{\partial m} (r^2 U) + V^2 S. \quad (2)$$

Here  $S(r,t)$  is the source, describing loss of material due to burnup due to thermalization of fast particles:

$$S = -\sum_{ik} n_i n_k \langle \sigma_{ik} v \rangle (m_i + m_k) + \sum_j N_j M_j,$$

where  $\sigma_{ik}$  is the cross section for the reaction between plasma nuclei of species  $i$  and  $k$ , and  $N_j$  is the number of fast particles of species  $j$  thermalized per unit volume.

The equations for ion and electron energy balance in the one-fluid two-temperature hydrodynamic approximation take the form<sup>5</sup>

$$\begin{aligned} C_e \frac{\partial T_e}{\partial t} + P_e \left( \frac{\partial V}{\partial t} - V^2 S \right) + \frac{\partial q_e}{\partial m} + \frac{T_e - T_i}{\rho \tau_T} &= Q_{Re}, \\ C_i \frac{\partial T_i}{\partial t} + P_i \left( \frac{\partial V}{\partial t} - V^2 S \right) + \frac{\partial q_i}{\partial m} - \frac{T_e - T_i}{\rho \tau_T} &= Q_{Ri}. \end{aligned} \quad (3)$$

Here  $C_e$  and  $C_i$  are the specific heats of the electrons and ions,  $T_e$  and  $T_i$  are the electron and ion temperatures,  $q_e = -\kappa_e \rho r^4 \partial T_e / \partial m$ ,  $q_i = -\kappa_i \rho r^4 \partial T_i / \partial m$  are the electron and ion thermal conduction fluxes,  $Q_{Re}$ ,  $Q_{Ri}(\rho, T_e, T_i)$  is the specific energy imparted to the ions and electrons of the plasma by fast reaction products, and  $\tau_T(\rho, T_e)$  is the characteristic time for energy exchange between ions and electrons.

The dissipation rates (divergences of fluxes) for energy, momentum, and particle number are  $Q_{Re}$ ,  $Q_{Ri}$ ,  $F$ , and  $N_j$ ; they are given in terms of the known particle distribution functions  $f_j(v, r, \mu)$  by the relations

$$\begin{aligned} Q_{Re, Ri} &= 2\pi \sum_j \int m_j a_{e,i} f_j v^3 d\mu dv, \\ F &= 2\pi \sum_j \int m_j (a_e + a_i) f_j v^2 dv \mu d\mu, \\ N_j &= 2\pi \lim_{v \rightarrow 0} \left\{ (a_e + a_i) v^2 \int f_j d\mu \right\}, \end{aligned} \quad (4)$$

where  $\mu$  is the cosine of the angle between the radius vector and the particle velocity,  $a_e \equiv dv/dt|_e$ ,  $a_i \equiv dv/dt|_i$  are the Coulomb drag terms for a fast particle due to electrons and ions respectively, and  $m_j$  is a particle mass.

The quasisteady kinetic equations for the distribution functions  $f_j$  of the fast ions and  $f_n$  of the neutrons take the form<sup>5,6</sup>

$$\begin{aligned} v \left( \mu \frac{\partial}{\partial r} + \frac{1 - \mu^2}{r} \frac{\partial}{\partial \mu} \right) f_n &= W_0 + W_{ns} - v f_n \sum_k n_k \sigma_{nk}, \\ v \left( \mu \frac{\partial}{\partial r} + \frac{1 - \mu^2}{r} \frac{\partial}{\partial \mu} \right) f_j + \frac{1}{v^2} \frac{\partial}{\partial v} (v^2 a_j f_j) &= W_0 + W_s \\ &\quad - v f_j \sum_k n_k \sigma_k. \end{aligned} \quad (5)$$

Here  $W_0(\rho, T, v)$ ,  $W_s, W_{ns}(r, v, \mu, \{f_n, f_j\})$  are the sources of initial thermonuclear particles and recoil nuclei from elastic scattering of thermonuclear neutrons,  $\sigma_k(r, v)$  and  $\sigma_{nk}(r, v)$  are the cross sections for secondary thermonuclear reactions between fast particles and plasma nucleons and for elastic scattering of neutrons on plasma nuclei,  $n_k$  is the density of nuclei of species  $k$ , and  $a_j(\rho, T, v) = a_{je} + a_{ji}$  is the Coulomb slowing-down rate.

Equations (5) describe the kinetics of charged and neutral thermonuclear reaction products, taking into account their Coulomb slowing down, elastic scattering, and secondary reactions with nuclei of the background plasma. Equations (1)–(5) constitute a closed system, the solution of which yields a model description of the dynamics of the thermonuclear burning of the plasma.

### 2.2. Choosing an object to study

As shown in Ref. 1, targets in which the mass in the active region is  $M_a \approx 10^{-3}$  g, for which a value  $\rho R > 2$  g/cm<sup>2</sup> can be achieved, are promising for experiments with laser energies  $E_L > 1$  MJ. A high burning efficiency  $K \sim 200$ –500 can be achieved if the temperature of the central burning region (igniter) is  $T_f = 10$ –20 keV and the mass is  $m_f \sim 10^{-1}$ – $10^{-2} M_a$ . In addition, as can be seen from calculations for direct compression of balloon targets,<sup>1,2,16–19</sup> the pressure in the core of the target at maximum compression is approximately constant.

Based on these ideas, we choose as the object of our investigation a model target with the following parameters at

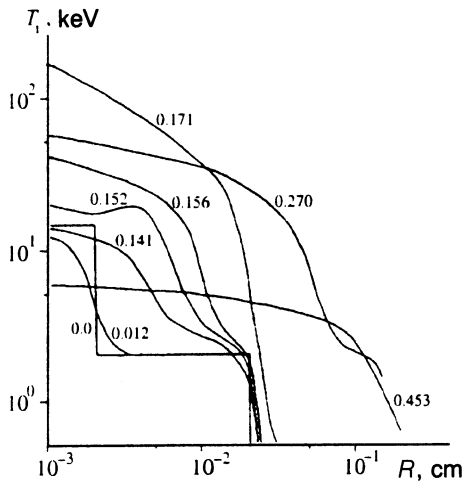


FIG. 1. Radial ion temperature profiles  $T_i(r, t)$  at various times in ns, revealing the propagation of the thermonuclear burn in a model shell-free DT target with an isobaric igniter at the time of maximum compression.

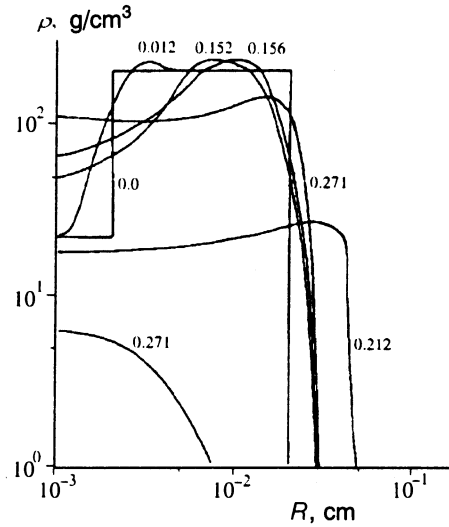


FIG. 3. Radial density profiles  $\rho(r, t)$  at various times in ns, revealing the disassembly of a model shell-free target with an isobaric igniter at the time of maximum compression.

maximum compression, employed as initial conditions:<sup>5</sup> the radii of the active zone and igniter are  $R_a=200 \mu\text{m}$ ,  $R_{f0}=20 \mu\text{m}$ , the temperature and density of the igniter are  $T_f=15 \text{ keV}$ ,  $\rho_f=25 \text{ g/cm}^3$ , and of the cold DT plasma are  $T_a=2 \text{ keV}$ ,  $\rho_a=200 \text{ g/cm}^3$ .

The radial profiles of the electron and ion temperatures and the plasma density at various times are plotted in Figs. 1–3, displaying the process by which the thermonuclear burning wave and the expansion of the cell-free DT target take place.<sup>5</sup> Figure 4 shows the time dependence of the ion scale temperature  $T_i(0, t)$ , the electron scale temperature  $T_e(0, t)$ , and the burning wave front radius  $R_f(t)$ .

By analyzing Figs. 1–4 we can distinguish two main stages in the development of the burning wave with isobaric initial conditions.

The first stage is that in which the wave formation is characterized by a low propagation speed  $\dot{R}_f < 5 \cdot 10^7 \text{ cm/s}$  and a temperature which falls off or grows slowly behind the front. Essentially there is no self-sustaining burn.

The second stage is the one in which the fully developed wave or “flare” develops, when  $\rho R_f$  and  $T_f$  attain values such that the energy release in the burning zone exceeds the energy losses due to thermal conduction. This stage is characterized by the violation of the isobaric conditions, a rapid rise in temperature, and a high speed of propagation  $\dot{R}_f \sim 5 \cdot 10^8 - 10^9 \text{ cm/s}$  of the front, exceeding the velocity  $\dot{R}_0$  at which the target expands and the sound speed behind the front.

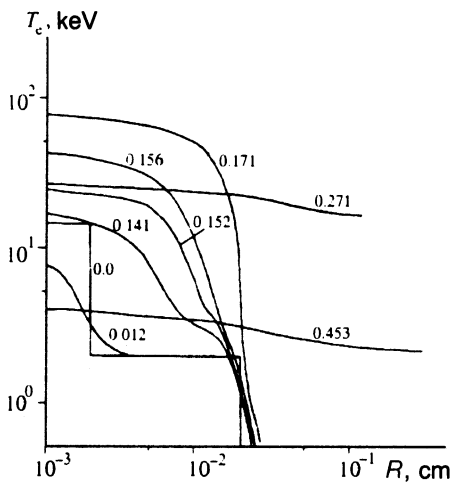


FIG. 2. Radial electron temperature profiles  $T_e(r, t)$  at various times in ns, revealing the propagation of the thermonuclear burn in a model DT target with an isobaric igniter at the time of maximum compression.

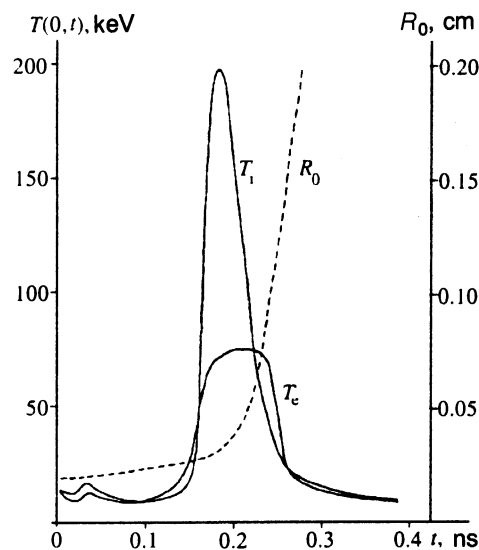


FIG. 4. Time dependence of the ion and electron temperatures  $T_i(0, t)$  and  $T_e(0, t)$  at the target center (solid trace) and also of the total radius  $R_0(t)$  of the model target (broken trace) in the burning stage and in the expansion, starting at the time of maximum compression.

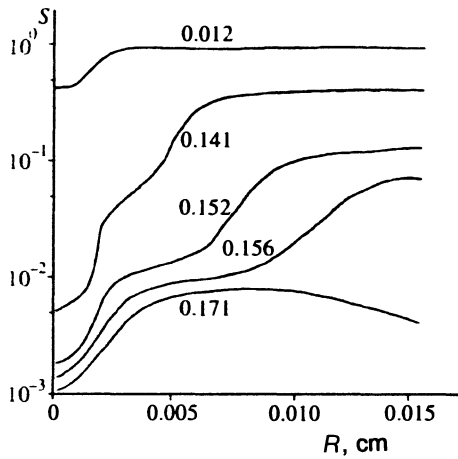


FIG. 5. Radial profiles of the ion—electron energy exchange intensity factor  $S(\rho, T_i, T_e)$  at various times in nanoseconds, corresponding to the development of a burn wave in the model target.

After the wave passes the target continues to burn for some time, but because of the sharp increase in the velocity  $\dot{R}_0$  the burning quickly quenches, and a stage of cooling and target expansion sets in.

### 2.3. Analysis of the numerical calculations

The principal advantage of the Monte Carlo method employed in the TERA code is the possibility of making a detailed study of the local properties of energy and momentum transport for the products of the thermonuclear reactions.

Let us consider the ion-electron energy exchange in the target. As a measure of the intensity of the energy exchange we introduce the factor

$$S(\rho, T_e, T_i) = 1 - \exp(-\Delta t_g / C_{ie} \rho \tau_T), \quad (6)$$

where  $\Delta t_g \sim 0.5 \min(C_e T_e / Q_{Re}, C_i T_i / Q_{Ri})$  is the typical time on which the plasma temperature changes,  $C_{ie} \rho \tau_T$  is the characteristic time for energy exchange between ions and electrons, and  $C_{ie} = C_i C_e / (C_i + C_e)$ .

Radial profiles of the energy exchange factor  $S$  at times corresponding to the numerical experiment described above are shown in Fig. 5. Active energy exchange ( $S \sim 1$ ) occurs in the wave formation stage for  $T_f < 15$  keV. When the wave is fully developed energy exchange can be neglected ( $S \ll 1$ ) and the ion and temperature profiles develop relatively independently.

Let us consider energy transport by thermonuclear particles and plasma electrons. Radial profiles of the energy loss rate of the thermonuclear particles in the calculation per particle of the background plasma,  $Q_R \equiv (Q_{Re} + Q_{Ri}) / (C_e + C_i)$ , and the divergence of the thermal conduction flux  $Q_e \equiv i / C_i + C_e \partial q_e / \partial m$  are displayed in Fig. 6. From Fig. 6 it follows that in the initial stage energy transport at the front ( $r \sim R_f$ ) and consequently the wave propagation speed, are determined mainly by energy losses of the charged particles,  $Q_R > Q_e$ . When the wave is fully developed the primary mechanism at the front is thermal conduction:  $Q_R < Q_e$ , and the energy loss by fast particles outside the burning region can be disregarded.

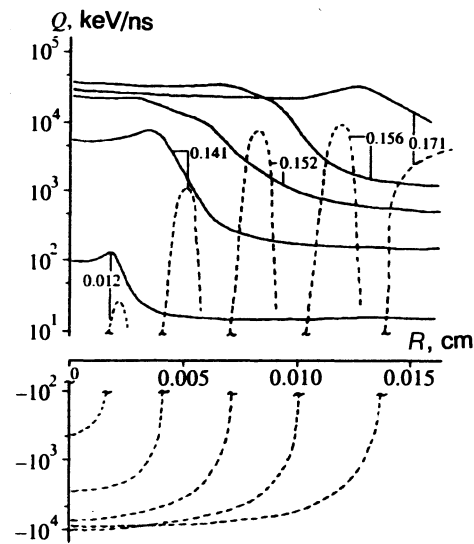


FIG. 6. Radial profiles of the energy dissipation (divergence of the fluxes) per particle in the medium in the calculation due to the mechanisms of electron thermal conduction  $Q_e$  nanoseconds (broken trace) and fast-particle energy losses  $Q_R$  (solid trace) at various times in ns, corresponding to a burn wave in the model target.

The sign of the total energy dissipation rate behind the wave front ( $r \ll R_f$ ) determines the condition for self-ignition of the target. For  $Q_R > |Q_e|$  the burning wave is self-sustaining and the temperature  $T_f$  grows behind the front; for  $Q_R < |Q_e|$  it damps. Thus, in the wave-formation stage in the region behind the front we usually have  $Q_R < |Q_e|$  and  $\dot{T}_f < 0$ .

We introduce the parameters  $f_R(\rho R_f, T_f) = Q_R / |Q_e|_{r=R_f}$ ,  $f_0(\rho R_f, T_f) = Q_R / |Q_e|_{r=0}$ , which depend on the dimension  $\rho R_f$  of the front and the temperature  $T_f$  behind the front. The parameter  $f_R$  shows which energy transport mechanism determines the velocity of the burning wave for given values of  $\rho R_f$  and  $T_f$ . For  $f_R > 1$  the main transport mechanism is via particles; for  $f_R < 1$  it is through thermal conduction. The parameter  $f_0$  determines the condition for self-ignition of the target for given values of  $\rho R_f$  and  $T_f$ . For  $f_0 > 1$  the wave is characterized by a temperature that increases behind the front, while for  $f_0 < 1$  it falls off.

The conditions  $f_R(\rho R_f, T_f) = 1$ ,  $f_0(\rho R_f, T_f) = 1$  divide the  $(\rho R_f, T_f)$  plane into regions in which a burning wave is possible with the corresponding properties. These regions, which were obtained as a result of the numerical simulation using the TERA code in a series of uniform-density model targets in Ref. 6, are shown in Fig. 7.

As a result we can draw the following conclusions about the typical behavior of the thermonuclear burning wave in the various stages of its development, needed in order to choose an approximate physical model of the thermonuclear burn of a laser target when the laser energy is  $< 10$  MJ, and in the subsequent analysis carried out analytically:

1. When the burning is fully developed the velocity of the wave front is considerably greater than the average hydrodynamic speed  $\langle u \rangle$  behind the front,  $\dot{R}_f / \langle u \rangle \sim 5-7$ . When the wave is forming we have  $\dot{R}_f / \langle u \rangle \sim 1-2$ . The plasma re-

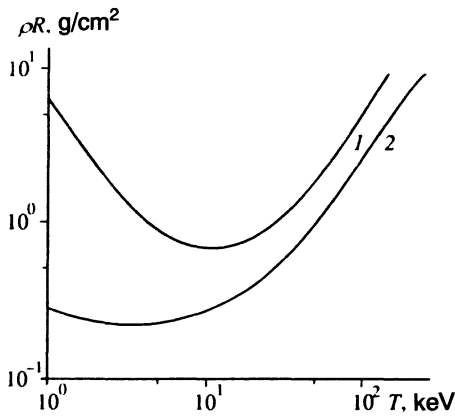


FIG. 7. Range of temperature  $T$  and  $\rho R$  within which burning occurs, where one of the energy transport mechanisms dominates: above trace 1 ( $f_R > 1$ ) fast-particle energy losses dominate at the boundary of the burning region, determining the thermonuclear wave velocity; below the trace ( $f_R < 1$ ) electron thermal conduction dominates. Above trace 2 ( $f_0 > 1$ ) in the burning region fast-particle heating dominates; below the trace ( $f_0 < 1$ ) cooling due to thermal conduction dominates.

mains approximately isobaric and the motion of the material has a substantial effect on the duration of this stage. Thus, an adequate description of energy transport in the target in the initial stage of the thermonuclear burning wave requires exact treatment of the motion of the material. When the wave is fully developed the motion of the target material can be disregarded and the wave propagates through the target with a velocity which is approximately constant.

Note that the conditions imposed on the parameters of the burning zone, shown in Fig. 7, apply specifically to the stage in which the wave is fully developed, when the stage of the target can be regarded as isochoric ( $\rho = \text{const}$ ); they cannot be employed to analyze the isobaric stage of wave formation.

2. In the formation stage the burning wave velocity determines the particle transport (cf. Fig. 6), and in the stage of fully developed burning at high temperatures the main contribution to the energy transport at the front comes from the electron thermal conduction (see Fig. 7). The effect of the fast particles on the wave velocity becomes averaged out through heating of the active zone of the target and nonlinear effects in the thermal conduction mechanism.

This means that in the stage when the wave is fully developed we can assume that the sources satisfy  $Q_{Re}$ ,  $Q_{Ri} \approx 0$  for  $r > R_f$  in the energy balance equations.

3. As can be deduced from Fig. 5, we can disregard energy exchange between ions and electrons in the plasma when the wave is fully developed.

It is evident that the duration of both the first and second stages is determined by the initial conditions at the instant of maximum compression. If the formation stage is prolonged, then the target may not ignite because of quenching of the heat or because the target blows apart.

Note also that, as shown by the numerical calculations using the TERA code, the fully-developed-wave stage contributes up to 80–90% to the total gain  $K$ . Consequently, the calculation can reasonably be continued only until the wave

reaches the target boundary and the maximum target temperature is achieved, since the expansion stage yields only about 10–20% of the total energy release.

### 3. SELF-SIMILAR DESCRIPTION OF A FULLY DEVELOPED THERMONUCLEAR BURNING WAVE IN A SPHERICAL TARGET

#### 3.1. Formulation of the problem

Having in mind the main properties of a fully developed thermonuclear burning wave, we disregard the motion of the material, ion-electron energy exchange, and ion thermal conduction. As a result the system of energy balance equations (3) of an isochoric ( $\rho = \text{const}$ ) plasma can be written in the form

$$\frac{\partial T_e}{\partial t} - \frac{1}{r^2} \frac{\partial}{\partial r} \left( \kappa_0 r^2 T_e^n \frac{\partial T_e}{\partial r} \right) = Q_e, \quad (7)$$

$$\frac{\partial T_i}{\partial t} = Q_i,$$

where  $Q_i$  and  $Q_e$  are the rates of energy production from the thermonuclear particles and  $\kappa_0 T_e^n$  is the thermal conduction coefficient; in an ideal Maxwellian plasma we set  $n = 5/2$ .

Equations (7) in general constitute an integrodifferential set, since the sources  $Q_e$  and  $Q_i$  depend on time through the nonlinear functionals (4) of the temperature profile,  $Q(r, t) = Q(\{T(r', t)\}, r)$ . Here it is understood that we integrate over the primed variables.

Note that, as mentioned above, when the wave is fully developed the dominance of the divergence of the thermal conduction flux at the front implies that the region where the sources  $Q_e$  and  $Q_i$  act can be regarded as bounded by the wave front  $R_f$ . This condition is a prerequisite for using a self-similar approach to solve the system of energy balance equations (7).

To transform to the self-similar description we represent the space-time dependence of the wave temperature  $T(r, t)$  and the source  $Q(r, t)$  as separable functions:

$$\begin{aligned} T_e(r, t) &= T_e(t) \Phi_e(\tau); & T_i(r, t) &= T_i(t) \Phi_i(\tau), \\ Q_e(r, t) &= Q_e(t) q_e(\tau); & Q_i(r, t) &= Q_i(t) q_i(\tau), \end{aligned} \quad (10)$$

where  $\tau = r/R(t)$ .

The question regarding the physical conditions under which the approximate factorization of the source is justified will be treated below in Sec. 3.4.

Here we assume that the ion and electron temperature fronts have radii that are equal or proportional:  $R_e(t)/R_i(t) = \text{const}$ . The reason for this is that, since the velocity of the front is determined by the electron thermal conductivity, the region in which the fast particles move is bounded by the electron temperature front. On the other hand, the energy losses of the thermonuclear particles on the ions, which determine the rate at which the ion temperature increases and consequently the rate of thermonuclear energy release, do not depend on temperature.

Hence, as noted above, if the wave front velocity is less than the speed of the fast particles, then the burning region which is determined by the ion temperature front should be the same as the electron temperature front.

If we assume that there exists a self-similar solution of the form (10), we can write the system of partial differential equation (7) as a system of ordinary differential equations:

$$\begin{aligned} \Phi_e - \frac{\dot{R}T_e}{RT_e} \tau \Phi_e' - \frac{T_e^{n+1}}{R^2 T_e} \kappa_0 \tau^{-2} (\tau^2 \Phi_e^n \Phi_e')' &= \frac{Q_e}{T_e} q_e, \\ \Phi_i - \frac{\dot{R}T_i}{RT_i} \tau \Phi_i' &= \frac{Q_i}{T_i} q_i. \end{aligned} \quad (11)$$

A necessary condition for the existence of a self-similar solution is that the coefficients of the functions  $\Phi(\tau)$  and  $q(\tau)$  be constant:

$$\dot{R}T_e/R\dot{T}_e = A_e, \quad \dot{R}T_i/R\dot{T}_i = A_i, \quad (12)$$

$$\kappa_0 T_e^n / \dot{R}R = B, \quad (13)$$

$$Q_e / \dot{T}_e = S_e, \quad Q_i / \dot{T}_i = S_i, \quad (14)$$

where  $A_e, A_i, B, S_e, S_i = \text{const}$ . When conditions (12)–(14) hold the system (11) assumes the form

$$\Phi_e - \tau A_e \Phi_e' - A_e B \tau^{-2} (\tau^2 \Phi_e^n \Phi_e')' = S_e q_e, \quad (15)$$

$$\Phi_i - \tau A_i \Phi_i' = S_i q_i \quad (16)$$

with boundary conditions

$$\Phi_e(0) = \Phi_i(0) = q_e(0) = q_i(0) = 1, \quad (17)$$

$$\Phi_e(1) = \Phi_i(1) = 0. \quad (18)$$

### 3.2. Self-similar solution for a two-temperature wave

The parameter  $S_i$ , which satisfies condition (17), assumes the value  $S_i = \Phi_i(0)/q_i(0) = 1$ , and Eq. (16) admits the solution

$$\Phi_i(\tau) = \frac{\tau^{1/A_i}}{A_i} \int_{\tau}^1 q(s) s^{-1-1/A_i} ds. \quad (19)$$

For a uniform source  $q_i(\tau) = 1$  the function  $\Phi_i(\tau)$  takes the simple form

$$\Phi_i(\tau) = 1 - \tau^{1/A_i}, \quad A_i > 0. \quad (20)$$

We obtain the numerical solution of Eq. (15) by integrating (15) twice, taking into account the boundary conditions (17) and (18):

$$\begin{aligned} \Phi_e(\tau)^{n+1} &= 1 - F \int_0^{\tau} \left[ \left( \Phi_e - q_e \frac{I_f^2}{I_q^2} \right) s - \left( C \Phi_e - q_e \frac{I_f^2}{I_q^2} \right) \tau \right] \frac{s ds}{\tau} \\ S_e &= (2A_e + 1) I_f^2 / I_q^2. \end{aligned} \quad (21)$$

Here  $F(\{\Phi\}, \{q\}, A_e) = 1 / (I_f^2 I_q^1 / I_q^2 - C I_f^1)$  is a functional of the wave profile  $\Phi(\tau)$  and the source  $q(\tau)$ , and we have written  $q(\tau)$ ,  $C = (2A_e + 1) / (3A_e + 1)$  and  $I_f^1 \{f\} = \int_0^1 f(s) s^n ds$ . For a uniform source ( $q \sim 1$ ) expressions (21) simplify:

$$\Phi_e^{n+1}(\tau)^{n+1} = 1 - F \left[ \frac{\tau^2}{2} I_f^2 + \int_0^{\tau} \Phi_e(s) \left( \frac{s}{\tau} - C \right) s ds \right], \quad (22)$$

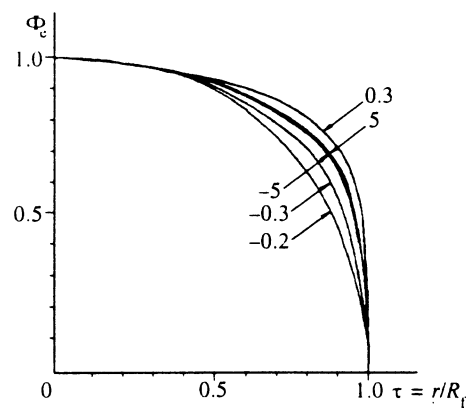


FIG. 8. Wave temperature profiles  $\Phi_e(t)$  in the self-similar variables for different values of the parameter  $A_e$ , calculated by the method of successive approximations.

$$S_e = 3(2A_e + 1) I_f^2,$$

where  $F = 1 / (1.5 I_f^2 - C I_f^1)$ .

From Eq. (22) we find asymptotic forms for the self-similar wave profile  $\Phi_e(\tau)$  at the boundary and in the center of the burning zone:

$$\Phi_e(\tau) = [nF(1-C)(1-\tau)/(n+1)]^{1/n}, \quad \tau \rightarrow 1, \quad (23)$$

$$\Phi_e(\tau) = 1 - \frac{\tau^2}{2(n+1)} F(I_f^2 + 2/3 - C), \quad \tau \rightarrow 0. \quad (24)$$

From (23) it follows that for a solution to exist the condition  $F(1-C) > 0$  must hold; this is satisfied in the range of the parameter  $A_e$  given by:

$$A_e < 0, \quad A_e > (2I_f^1 - 3I_f^2) / (9I_f^2 - 4I_f^1). \quad (25)$$

The solution of Eq. (22) by iteration for different values of the parameter  $A_e$  is shown in Fig. 8. Table I gives values of the parameters  $F, S_e, I_f^1$ , and  $I_f^2$  and of the parameter  $B = (3A_e + 1)(n+1)/A_e F$  from condition (13); these are functionals of the profile  $\Phi_e$ . For  $0 < A_{ei} < 0.2$  the iterations fail to converge, which follows from (25).

### 3.3 Conditions for self-similarity

Consider the self-similarity conditions (12)–(14), which establish a relation between the wave scales  $R(t), T(t)$  and that of the source  $Q(t)$ .

TABLE I. Numerical values of functionals  $I_f^n, S_e, F$ , and  $B$  [Eqs. (15) and (16)] as functions of the temperature profile  $\Phi_e$  for different values of the similarity parameter  $A_e$ .

$A_e$	$I_f^1$	$I_f^2$	$S_e$	$F$	$B$
5.00	0.389	0.241	11.6	10.5	1.06
1.00	0.395	0.246	2.95	13.6	1.03
0.30	0.410	0.258	1.47	23.3	0.95
-0.20	0.336	0.196	0.235	-4.76	1.47
-0.50	0.371	0.226	-0.339	2.95	1.19
-5.00	0.386	0.239	-10.2	9.09	1.08

Condition (12) corresponds to the statement that the radius of the front is a power-law function of the temperature behind the front:

$$R(t)/R_0 = (T_e(t)/T_{e0})^A = (T_i(t)/T_{i0})^A, \quad (26)$$

where  $R_0 = R(0)$ ,  $T_{e0} = T_e(0,0)$ ,  $T_{i0} = T_i(0,0)$ .

Conditions (12) and (13) yield an explicit form for the dependences  $R(t)$  and  $T_e(t)$ :

$$\begin{aligned} R(t) &= R_0(1 + t/bt_0)^b, \\ T_e(t) &= T_{e0}(1 + t/bt_0)^a, \end{aligned} \quad (27)$$

where  $b = A_e/(2A_e - n)$ ,  $a = b/A_e = 1/(2A_e - n)$ ,  $t_0 = BR_0^2/\kappa_0 T_{e0}^n$ .

It follows from (27) that two kinds of solution are possible: an algebraic regime for  $b > 0$ , and also a hyperbolic regime or "intensified regime" for  $b < 0$  in which the wave scales  $T(t)$  and  $R(t)$  diverge over a finite time interval  $|b|t_0$ . A detailed classification of the enhanced regimes is given in Ref. 15.

Condition (14) imposes a restriction on the form of the temperature dependence of the source scale for the electron temperature  $Q_e(T_e)$ :

$$Q_e(T_e) = Q_{e0}(T_e/T_{e0})^s, \quad (28)$$

where  $Q_{e0} = S_e T_{e0}/A_e t_0$ ,  $s = n + 1 - 2A_e$ .

If the function  $Q_e(T_e)$  is taken to be of the form (28), then the self-similar parameters  $A_e$ ,  $b$ ,  $a$ , and  $t_0$  can be expressed in terms of the source parameters  $s$  and  $Q_{e0}$ :

$$\begin{aligned} A_e &= \frac{1}{2}(n + 1 - s), \quad b = \frac{1}{2} \left( 1 + \frac{n}{1 - s} \right), \\ a &= \frac{b}{A_e} = \frac{1}{1 - s}, \quad t_0 = S_e T_{e0}/A_e Q_{e0}. \end{aligned} \quad (29)$$

At the same time the parameter  $s$  determines the behavior of the power-law dependence of the front radius and temperature of the self-similar burning wave,  $Q_{e0}$  provides a connection between the coefficients  $R_0$  and  $T_{e0}$ , which determine the set of possible self-similar wave trajectories  $R(T_e)$  consistent with the given source intensity  $Q_{e0}$ :

$$R_0^2 = D T_{e0}^{n+1}/Q_{e0}, \quad (30)$$

where  $D = S_e \kappa_0/A_e B$ .

Note that, in contrast to  $A_e$ , the parameter  $A_i$  that determines the ion temperature profile  $\Phi_i(\tau)$  cannot be derived from the form of the source  $Q_i$ . Hence in order to find  $A_i$  we need to establish a relation between the electron and ion temperatures,  $T_i = T_i(T_e)$ . Then the condition for the fronts (26) to be equal determines the relation between  $A_e$  and  $A_i$ .

For this purpose we consider in more detail the behavior of the sources  $Q_e$  and  $Q_i$  as functions of  $T_e$  and  $T_i$ . Using (8) and (9) we express the total rate of energy losses of the thermonuclear particles per unit volume  $Q = Q_e + Q_i$  in the form

$$Q(T_e, T_i, R) = W(T_i) E_0 \eta(T_e, \rho R). \quad (31)$$

We approximate the temperature dependence of the particle mean free path as

$$1/\lambda(T_e) = 1/\lambda_i + 1/\lambda_e(T_e), \quad (32)$$

where  $\lambda_i = \text{const}$ , and  $\lambda_e(T_e) = \lambda_{e0}(T_e/T_{e0})^{3/2}$  are the particle mean free paths when ion or electron energy losses alone are present. Then the sources  $Q_i$  and  $Q_e$  can be represented approximately in the form

$$Q_e = Q\lambda/\lambda_e, \quad Q_i = Q\lambda/\lambda_i. \quad (33)$$

Using relation (14) together with (33) we write

$$\lambda_e(T_e)/\lambda_i = Q_i/Q_e = \dot{T}_i/\dot{T}_e S_e. \quad (34)$$

Hence, using the temperature dependence  $\lambda_e(T_e)$  we find

$$T_i(T_e) = T_{i0} + g T_{e0} [(T_e/T_{e0})^{5/2} - 1], \quad (35)$$

where  $g = 2S_e \lambda_{e0}/5\lambda_i$ .

From (35) it follows that for a wave with increasing electron temperature ( $A_e > 0, g > 0$ ) the ion and electron temperatures will be related after a certain time  $t_a$  by a simple power-law dependence,  $T_i \sim T_e^{5/2}$ . This time can be estimated from the relation

$$T_e(t)/T_{e0} > |1/g - 1|^{2/5}. \quad (36)$$

Using (27) and taking into account that in the plasma when the temperature is sufficiently high we have  $g > 1$ , we find for the power-law regime ( $b > 0$ ) that  $t_a \sim bt_0$  holds, while for the enhanced regime ( $b < 0$ ) we have  $t_a \sim |b|t_0/2$ .

When the electron temperature is damping ( $A_e < 0, g < 0$ ) the ion temperature varies over the range  $T_{i0} < T_i < T_{i0} + |g|T_{e0}$ . Here there is no power-law dependence in  $T_i(T_e)$ , but if  $|g| \gg 1$  holds (e.g., at high temperatures when we have  $\lambda_{e0} \gg \lambda_i$ ), then over finite ranges of  $T_e$  we can assume approximately  $T_i \sim T_e^k$ ,  $-5/2 < k < 0$ .

### 3.4. Self-similar regimes of burning wave propagation

Condition (28) requires a power-law dependence  $Q_e \sim T_e^s$ . Hence for the self-similar burning regime to hold it is rigorously necessary that all quantities entering into the definition (31), (33) depend algebraically on  $T_e$ :

$$T_i(T_e) \sim T_e^k, \quad W(T_i) \sim T_i^m, \quad \lambda(T_e) \sim T_e^d, \quad \eta(T_e) \sim T_e^r. \quad (37)$$

As noted previously, the occurrence of the power-law dependence  $T_i(T_e)$  is possible after a time interval  $t_a$  which is the characteristic time for the self-similar regime to be established.

In a uniform plasma the burning velocity  $W$  and propagation distance  $\lambda$  depend only on temperature, while the energy fraction  $\eta$  also depends on the size of the front. In the general case  $\eta(R, T_e)$  is not an algebraic function of  $T_e$ . The self-similar description of burning is possible in the following asymptotic cases:

1. The burning region is transparent for fast waves ( $R \ll \lambda$ )

$$\eta \sim R/\lambda \ll 1, \quad r = A_e - d.$$

2. The burning region is opaque for fast waves ( $R > \lambda$ )

$$\eta \sim 1, \quad r = 0.$$

Finally, using (29) and (33) we find expressions for the parameters  $a$ ,  $b$ ,  $s$ , and  $A_e$  which determine the temperature and time dependence of the scale quantities  $R$ ,  $T_e$ , and  $T_i$  of the burning wave in accordance with (27):

$$\begin{aligned} \eta \ll 1: \quad & s = (2/3)(km + n/2 - 1), \\ & A_e = (n + 5/2 - km)/3, \\ & b = (1/2)(1 + 3n/(5 - 2km - n)), \end{aligned} \quad (38)$$

$$\begin{aligned} \eta \sim 1: \quad & s = km + d - 3/2, \\ & A_e = (n + 5/2 - km - d)/2, \\ & b = (1/2)(1 + n/(5/2 - km - d)), \\ & A_i = A_e/k, \quad a = b/A_e. \end{aligned} \quad (39)$$

Here, corresponding to (32), we have  $0 < d < 3/2$ .

As follows from the numerical calculations, in the temperature range  $T_e < 15$  keV the ion-electron energy exchange increases sharply, and the plasma becomes one-temperature:  $A_e = A_i = A$ ,  $\Phi_e = \Phi_i = \Phi$ ,  $k = 1$ . When energy losses from fast thermonuclear particles on electrons dominate ( $\lambda = \lambda_e \sim T_e^{3/2}$ ) the  $\Phi(\tau)$  profile is determined by Eqs. (15) and (22). Thus, if we set  $k = 1$ ,  $d = 3/2$  then relations (38) and (39) also hold for the case of a one-temperature plasma.

Finally, we write down the behavior of the self-similar parameters  $s$ ,  $b$ ,  $a$ , and  $A_e$  as functions of the power-law index  $m$  in the temperature dependence of the thermonuclear reaction rate for an ideal ( $n = 5/2$ ) plasma.

1. One-temperature plasma ( $k = 1$ ,  $d = 3/2$ ,  $A_e = A_i = A$ ):

$$\begin{aligned} \eta \ll 1: \quad & s = 2(m + 0.25)/3, \\ & A = (5 - m)/3, \\ & b = 0.5(1 + 3/(1 - 0.8m)), \\ & a = 1.2/(1 - 0.8m), \\ \eta \sim 1: \quad & s = m, \\ & A = 1.75 - 0.5m, \\ & b = 0.5(1 + 2.5/(1 - m)), \\ & a = 1/(1 - m). \end{aligned} \quad (40)$$

2. Two-temperature plasma ( $k = 5/2$ ,  $0 < d < 3/2$ ,  $A_i = A_e/k$ ):

$$\begin{aligned} \eta \ll 1: \quad & s = (10m + 1)/6, \\ & A_e = 5(2 - m)/6, \\ & b = 0.5(1 + 3/(1 - 2m)), \\ & a = 1.2/(1 - 2m), \\ \eta \sim 1: \quad & s = 2.5m - 1.5 + d, \\ & A_e = (5 - 2.5m - d)/2, \\ & b = 0.5(1 + 1/(1 - m - 0.4d)), \\ & a = 0.4/(1 - m - 0.4d). \end{aligned} \quad (41)$$

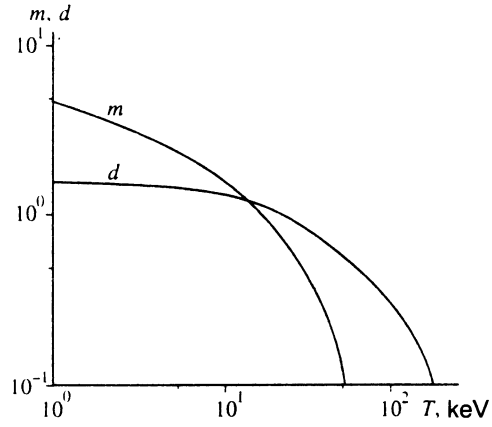


FIG. 9. Temperature dependence of the power-law indices  $m(T)$  and  $d(T)$  in the approximate power-law functions for the thermonuclear reaction rate  $\langle \sigma_{DT} v \rangle \sim T^m$  and the fast  $\alpha$ -particle path length to thermalization  $\lambda \sim T^d$ .

Note that the special case described by relations (41) was derived previously in Refs. 8 and 9.

### 3.5. Conditions for the development of a self-similar burning regime in deuterium-tritium plasma

In a real plasma the parameters  $m$  and  $d$  are functions of temperature,  $m = m(T_i)$  and  $d = d(T_e)$ . In an ideal Maxwellian DT plasma in the temperature range  $1 < T < 100$  keV the parameters  $m$  and  $d$  vary over the range  $4 > m > 0$  and  $1.5 > d > 0$ . The temperature dependence of these parameters for a DT plasma is shown in Fig. 9.

Using (40)–(43) and the function  $m = m(T)$ , we can estimate the temperature limits of the various self-similar burning regimes.

The condition for the propagation of a self-similar burning wave with increasing temperature, i.e.,  $A_e > 0$ , is satisfied in the region

$$\begin{aligned} (T_i = T_e): \quad & (T_i \neq T_e): \\ \eta \ll 1: \quad & m < 5, \quad m < 2 \\ \eta \sim 1: \quad & m < 7/2, \quad m < 2 - 2d/5 \sim 7/5. \end{aligned} \quad (44)$$

Since the one-temperature and two-temperature plasmas become distinct for  $T \sim 10$ – $15$  keV, which corresponds to  $m \sim 1.5$ – $2$  in a DT plasma, in a two-temperature DT plasma when the self-similar combustion regime holds only the regime with increasing temperature is possible. In a one-temperature isochoric plasma the self-similar regime with quenched burning is possible only at temperatures  $T < 5$  keV, for which there is no combustion in a real thermonuclear situation, and the wave propagation in accordance with Refs. 9 and 12 is determined by detonation.

The condition for the occurrence of the hyperbolic burning regime (the “enhanced regime”) is satisfied for the range of values of the parameter  $b < 0$ , which is determined by the boundaries of the parameter  $m$ :

$$\begin{aligned} (T_i = T_e): \quad & (T_i \neq T_e): \\ \eta \ll 1: \quad & 5/4 < m < 5, \quad 1/2 < m < 2, \end{aligned} \quad (45)$$

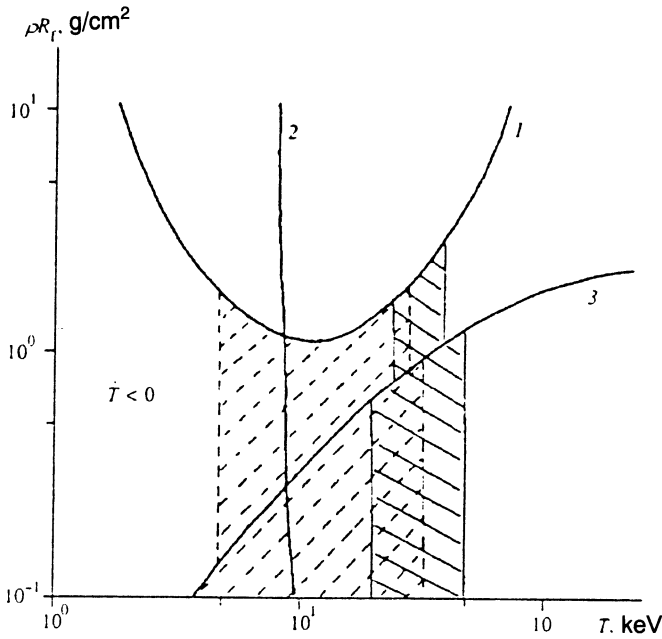


FIG. 10. Regions of temperature and  $\rho R$  for the burning zone in which different self-similar burning waves are possible. These self-similar solutions of the system of energy balance equations refer to the region below trace 1, where energy transport at the boundary of the burning zone is determined by thermal conduction. To the right of trace 2 in the burning zone  $T_i \neq T_e$  holds, while to the left  $T_i = T_e$  holds. Above trace 3 the radius of the burning zone is larger than the  $\alpha$ -particle mean free path ( $\eta \sim 1$ ); below it the burning region is transparent to  $\alpha$ -particles ( $\eta < 1$ ). In the region with dashed cross-hatching, the "enhanced region," to the left of the broken trace is the region where the self-similar wave is damped. In the region of solid cross-hatching no self-similar regime develops.

$$\eta \sim 1: \quad 1 < m < 7/2, \quad 1 - 2d/5 < m < 2 - 2d/5.$$

Note that the presence of the enhanced regime still does not imply fast burning. Thus, in the low-temperature regime when the energy release rate  $Q(t)$  is weak the time interval  $bt_0 = aS_e T_e / Q_e$  of the enhancement can be too large for the hyperbolic nature of the burning to manifest itself.

Let us consider the restrictions on the temperature and the dimensions of the front under which the self-similar burning regime (40)–(43) is possible. We will assume that the scales are the same,  $T_e(t) = T_i(t)$ , although the two-temperature nature of the burning is retained and the temperature profiles of the wave differ:  $\Phi_e(\tau) \neq \Phi_i(\tau)$ .

The main requirement for this problem to be physically well-posed is that the principal energy transport mechanism at the wave front, which determines its propagation speed, be electron thermal conduction. A curve analogous to Fig. 7, dividing the  $(\rho R, T)$  plane to regions in which electron and  $\alpha$ -particle thermal conduction dominates, is shown in Fig. 10.

The criterion for one- or two-temperature plasmas to exist can be derived by equating the fast-particle energy losses to the energy produced as a result of ion-electron energy exchange:

$$T/\tau_T(T) = E_0 W(T) \eta(\rho R, T). \quad (46)$$

The condition for dividing the regions in which the restrictions  $\eta \sim 1$  and  $\eta \ll 1$  hold is given by

$$\rho R = \rho \lambda(T). \quad (47)$$

The curves in the  $(\rho R, T)$  plane given by relations (46) and (47) are shown in Fig. 10.

Let us consider in more detail the condition for the self-similar burning regime to be established, and also for when it is possible to describe the propagation of the thermonuclear burn wave in the adiabatic approximation according to (27) with variable self-similar parameters  $a(T)$  and  $b(T)$ . For this it is necessary that the parameters  $a(T)$  and  $b(T)$  change little over the time  $t_a$  during which the regime is established.

In accordance with Figs. 9 and 10, the region in which the burning parameter  $m(T)$  varies rapidly extends to the region where the enhanced regime occurs, for which  $t_a \sim |b|t_0/2$  holds. Thus, using (14) we can write

$$\frac{1}{a} \frac{da}{dT}, \quad \frac{1}{b} \frac{db}{dT} \ll \frac{1}{Tt_a} = \frac{2S_e}{Q_e |b|t_0}. \quad (48)$$

Using (29) we can write condition (48) in the form

$$\frac{ds}{dT} \frac{T}{2(1-s)^2} < 1. \quad (49)$$

We can make condition (49) more specific by using relations (40)–(43) for the various self-similar burning regimes of a DT plasma:

$$(T_i \equiv T_e): \quad (T_i \neq T_e):$$

$$\eta \ll 1: \quad 3Tm'/(1.25 - m)^2 < 1,$$

$$0.3Tm'/(0.5 - m)^2 < 1, \quad (50)$$

$$\eta \sim 1: \quad 0.5Tm'/(1 - m)^2 < 1,$$

$$0.2Tx'/(1 - x)^2 < 1,$$

where  $x \equiv m + 0.4d$ ,  $m' \equiv dm/dT$ ,  $x' \equiv dx/dT$ .

Using the functions  $m(T)$  and  $d(T)$  for a DT plasma shown in Fig. 9, we find the temperature range in which the self-similar burning regime cannot develop because the self-similar parameters change too rapidly:

$$\eta \ll 1: \quad 20 < T < 50 \text{ keV},$$

$$\eta \sim 1: \quad 25 < T < 40 \text{ keV}. \quad (51)$$

The region in the  $(\rho R, T)$  plane in which the burning regime is not self-similar, corresponding to conditions (51), and also the regions where the "enhanced regime" occurs and the region where self-sustained burning occurs with a temperature that increases behind the front in accordance with Eqs. (44)–(47) are shown in Fig. 10.

#### 4. CONCLUSION

The foregoing analysis enables us to draw general conclusions about the behavior of self-similar thermonuclear burning waves in a two-temperature ideal DT plasma with uniform density.

• These self-similar regimes correspond to the conditions such that the energy transport at the front is determined by thermal conduction.

• The self-similar burning regime is possible either when the burning regime is relatively transparent for thermonuclear particles,  $\eta \sim R/\lambda \ll 1$ , or on the other hand when particles undergo considerable deceleration,  $\eta \sim 1$ ,  $R > \lambda$ .

• The self-similar regime is possible either in the form of a one-temperature wave or in the form of waves of ion and electron temperature coupled only by the overall dimensions of the front and the fractions of energy lost by the charged particles to ions and electrons.

• In the one-temperature regime in the region of realistic burning for a DT mixture,  $T > 5$  keV, and in the two-temperature regime the self-similar burning wave is characterized by a temperature that increases behind the front.

• In the region  $5 < T < 40$  keV in a DT plasma an “enhanced regime” is possible with  $T \sim 1/(t_0 - t)^a$ ,  $R \sim 1/(t_0 - t)^b$ ,  $t < t_0$ . In this regime the front velocity  $R$  is usually larger than in the power-law regime with  $T \sim t^a$ ,  $R \sim t^b$ . However, the behavior of the enhanced regime where  $T \rightarrow \infty$  for  $t \rightarrow t_0$  is not seen, since for  $T < 40$  keV the burning goes over to the power-law regime.

• The self-similar regime of thermonuclear burning develops when the self-similar parameters vary little over the characteristic time  $t_a$ .

Then it is possible to describe the burning wave using Eq. (27) in the adiabatic approximation for the variables  $a(T)$  and  $b(T)$ . In the opposite limit a self-similar regime cannot develop.

The regions in the  $(\rho R, T)$  plane in which the various burning regimes are possible, as well as the region in which the self-similar regime is unstable, are shown in Fig. 10. In the region of instability and close to the boundary where the different regimes are separated numerical simulation of the energy transport is necessary.

The most stable self-similar burning regime of a DT plasma forms in the region  $T_i > 40$  keV ( $m = 0$ ) with parameters

$$\eta \ll 1: \quad A_e = 5/3, \quad A_i = 2/3, \quad a_e = 6/5, \quad a_i = 3, \\ b = 2, \quad S_e = 13/3,$$

$$\eta \sim 1: \quad A_e = 5/2, \quad A_i = 1,$$

$$a_e = 2/5, \quad a_i = 1, \quad b = 1, \quad S_e = 6.$$

The time scale  $bt_0$  in a DT plasma for  $T_0 \sim 40$  keV and the energy of the thermonuclear particles  $E_0 = 3.5$  MeV have the values

$$bt_0 = a S_e T_0 \lambda_e / E_0 W \eta \lambda \approx 1.5 / \rho \eta \text{ [ns]},$$

where  $\rho$  is the plasma density in units of  $\text{g} \cdot \text{cm}^{-2}$ .

- <sup>1</sup> N. G. Basov, S. Yu. Gus'kov, G. V. Danilova *et al.*, *Kvantovaya Elektron.* (Moscow) **12**, 1289 (1985) [*Sov. J. Quantum Electron.* **15**, 852 (1985)].
- <sup>2</sup> E. N. Avrorin, A. I. Zuev, V. A. Lykov *et al.*, *Topics in Atomic Science and Technology*, Vol. 2, *Techniques and codes for numerical solution of mathematical physics problems* [in Russian].
- <sup>3</sup> J. H. Nuckols, in LLNL Laser Program Annual Report, 1979, Vol. 2, p. 21.
- <sup>4</sup> S. Yu. Gus'kov, A. A. Levkovskii, D. V. Il'in *et al.*, Lebedev Institute Preprint No. 68 (1990).
- <sup>5</sup> A. A. Levkovskii, Lebedev Institute Preprint No. 73 (1990).
- <sup>6</sup> O. B. Vygovsky, S. Yu. Gus'kov, D. V. Il'in *et al.*, *J. Soviet Laser Research* **14**(2), 85 (1993).
- <sup>7</sup> A. P. Nastoyashchii and L. P. Shevchenko, *Atomnaya Énerg.* **32**, 451 (1972).
- <sup>8</sup> S. Yu. Gus'kov, O. N. Krokhin, and V. B. Rozanov, *Nuclear Fusion* **16**, 957 (1976).
- <sup>9</sup> S. Yu. Gus'kov and V. B. Rozanov, in *Proceedings of the Lebedev Institute*, N. G. Basov (ed.), Vol. 134, p. 153 (1982).
- <sup>10</sup> M. A. Liberman and A. L. Velikovich, *J. Plasma Phys.* **31**, 381 (1984).
- <sup>11</sup> M. M. Basko and A. B. Bud'ko, Institute of Theoretical and Experimental Physics Preprint No. 27 (1986).
- <sup>12</sup> E. N. Avrorin, A. A. Bunatyan, and A. D. Gadzhiev, *Fiz. Plazmy* **10**, 514 (1984) [*Sov. J. Plasma Phys.* **10**, 298 (1984)].
- <sup>13</sup> P. P. Volosevich, S. P. Kurdyumov, and E. I. Levanov, *Zh. Prikl. Mekh. Tekh. Fiz.* No. 5, 41 (1972).
- <sup>14</sup> N. V. Zmitrenko, Institute of Applied Mechanics Preprint No. 159 (1989).
- <sup>15</sup> V. A. Galaktinov, V. A. Dorodnitsin, G. G. Elenin *et al.*, in *Current Problems in Mathematics*, Gamkrelidze (ed.), Vol. 28, p. 95 (1987).
- <sup>16</sup> R. E. Kidder, *Nuclear Fusion* **19**, 223 (1979).
- <sup>17</sup> R. J. Mason and R. L. Morse, *Nuclear Fusion* **15**, 935 (1975).
- <sup>18</sup> N. A. Tahir and K. A. Long, *Nuclear Fusion* **23**, 887 (1983).
- <sup>19</sup> N. Metzler and J. Meyer-ter Vehn, *Laser and Particle Beams*, Vol. 2, p. 27 (1984).

Translated by David L. Book